ARTICLE

Bone marrow-derived TNF-α causes diabetic neuropathy in mice

Hiroshi Urabe · Tomoya Terashima · Fan Lin ·
Hideto Kojima · Lawrence Chan

Abstract

Aims/hypothesis Dysregulation of biochemical pathways in response to hyperglycaemia in cells intrinsic to the nervous system (Schwann cells, neurons, vasa nervorum) are thought to underlie diabetic peripheral neuropathy (DPN). TNF-α is a known aetiological factor; *Tnf*-knockout mice are protected against DPN. We hypothesised that TNF-α produced by a small but specific bone marrow (BM) subpopulation marked by proinsulin production (proinsulin-producing BM-derived cells, PI-BMDCs) is essential for DPN development.

Methods We produced mice deficient in TNF-α, globally in BM and selectively in PI-BMDCs only, by gene targeting and BM transplantation, and induced diabetes by streptozotocin. Motor and sensory nerve conduction velocities were used to gauge nerve dysfunction. Immunocytochemistry, fluorescence in situ hybridisation (FISH) and PCR analysis of dorsal root ganglia (DRG) were employed to monitor outcome.

Results We found that loss of TNF-α in BM only protected mice from DPN. We developed a strategy to delete TNF-α specifically in PI-BMDCs, and found that PI-BMDC-specific loss of TNF-α protected against DPN as robustly as loss of total BM TNF-α. Selective loss of PI-BMDC-derived TNF-α downregulated TUNEL-positive DRG neurons. FISH revealed PI-BMDC−neuron fusion cells in the DRG in mice with DPN; fusion cells were undetectable in non-diabetic mice or diabetic mice that had lost TNF-α expression selectively in the PI-BMDC subpopulation.

Conclusions/interpretation BMDC-specific TNF-α is essential for DPN development; its selective removal from a small PI-BMDC subpopulation protects against DPN. The pathogenicity of PI-BMDC-derived TNF-α may have important therapeutic implications.

Abbreviations

BM	Bone marrow
BMT	BM transplantation
DPN	Diabetic peripheral neuropathy
DRG	Dorsal root ganglia
FISH	Fluorescence in situ hybridisation
KO	Knockout
MNCV	Motor nerve conduction velocity
PI-BMDC	Proinsulin-producing BM-derived cell
RIP	Rat insulin promoter
RIP-Cre	RIP-driven Cre
SNCV	Sensory nerve conduction velocity
STZ	Streptozotocin
Tnf-f	*Tnf*-floxed
WT	Wild-type

H. Urabe · T. Terashima · F. Lin · H. Kojima · L. Chan (✉)
Department of Medicine, Baylor College of Medicine, One Baylor Plaza (MS: BCM185), Houston, TX 77030, USA
e-mail: lchan@bcm.edu

H. Kojima · L. Chan
Department of Molecular and Cellular Biology, Baylor College of Medicine, Houston, TX, USA

H. Urabe · T. Terashima · H. Kojima
Department of Stem Cell Biology and Regenerative Medicine, Shiga University of Medical Science, Ōtsu, Japan

Introduction

Diabetic peripheral neuropathy (DPN) is a common complication of diabetes that afflicts more than half of all diabetic individuals [1–5]. The pathogenesis of DPN involves multiple aetiological factors downstream of hyperglycaemia, including oxidative stress [6, 7], increased mitochondrial production of reactive oxygen species [1], hypoxia [8], increased advanced glycation endproducts and the receptor RAGE [9, 10], activation of protein kinase C [11] and/or polyol pathways [12, 13], growth factor deficiency [14] and activation of inflammatory cytokines such as TNF-α and IL-6 [15]. These dysregulated pathways are thought to affect Schwann cells, neurons and vasa nervorum, cells and tissues intrinsic to the nervous system. There is, however, emerging evidence that bone marrow (BM)-derived haematopoietic cells contribute actively to the pathogenesis of DPN [16].

Our laboratory first described the presence of proinsulin-producing BM-derived cells (PI-BMDCs) in different tissues in rodent models of diabetes [17]. PI-BMDCs were shown to co-express TNF-α [18], an inflammatory cytokine that has been implicated in diabetic complications, including DPN [4, 19, 20]. Global inactivation of TNF-α either in knockout (KO) mice or by treatment with an anti-TNF-α monoclonal antibody was shown to ameliorate DPN [21]. Moreover, treatment with a recombinant human TNF-α receptor–antibody fusion protein partially ameliorates DPN in diabetic rats [22].

In diabetes, TNF-α is produced by many different cell types and tissues in the peripheral nervous system [4, 19, 20]. Here, we hypothesise that TNF-α produced by PI-BMDCs plays a determining role in the pathogenesis of DPN and that selective inhibition of TNF-α in PI-BMDCs only protects against DPN in diabetic mice. If proven correct, this is an important hypothesis because it identifies a specific cell target for therapeutic intervention.

Methods

Animals We purchased B6.129S-Tnf^{tm1Gkl}/J mice from Jackson Laboratories (Bar Harbor, ME, USA) and obtained $Tnf^{tm1.1Sned}$ mice from the US National Institutes of Health (Bethesda, MD, USA). B6.129S-Tnf^{tm1Gkl}/J mice were backcrossed to C57BL/6 mice for over 12 generations. *Tnf* floxed/RIP-Cre mice were produced by breeding transgenic *Tnf* floxed (*Tnf*-f) mice with rat insulin promoter (RIP)-driven Cre (RIP-Cre) mice [23–25]. For BM transplantation (BMT), we irradiated (10 Gy) 8-week-old C57BL/6J female mice and then injected 4×10^6 BM cells from male wild-type (WT) global *Tnf* KO mice or *Tnf*-f/RIP-Cre mice. At 4 weeks after BMT, we induced diabetes by intraperitoneal injection of streptozotocin (STZ; 150 mg/kg). The chimaerism of donor cells was >90% after 4 weeks and graft-vs-host-disease score

[26, 27] was very low. We used mice with blood glucose of >13.8 mmol/l on day 7 for study. All experiments were performed according to the guidelines of the Institutional Animal Care and Use Committee at Baylor College of Medicine.

Analysis of tissue mRNA and quantitative RT-PCR Total RNA was extracted by RNeasy Kit (Qiagen, Valencia, CA, USA) and treated with DNase I (Life Technologies, Carlsbad, CA, USA) digestion. After reverse transcription using oligo-dT primer (Life Technologies), the mRNA expression level of *Ins1*, *Ins2* and *Tnf* was quantified by real-time PCR using PerfeCta SYBR Green SuperMix, Low ROX and PerfeCta qPCR SuperMix (Quanta Biosciences, Gaithersburg, MD, USA). The primer sequences are listed in electronic supplementary material (ESM) Table 1. We used Mx3005P QPCR system (Stratagene, La Jolla, CA, USA), and results were analysed by MxProQPCR software, version 4.10 (Stratagene), using β-actin as control.

Immunohistochemical and immunocytochemical analysis We fixed the mice, after exsanguination, in 4% paraformaldehyde by perfusion and isolated dorsal root ganglia (DRG) at L3–L5. Isolated thigh bones were decalcified in 10% EDTA for one week. DRG and thigh bones were cut into 10 μm-thick sections and incubated with anti-proinsulin (mouse monoclonal; Fitzgerald Industries International, Acton, MA, USA), anti-TNF-α antibody (goat polyclonal; Santa Cruz Biotechnology, Dallas, TX, USA) and anti-microtubule-associated protein 2 (MAP2) antibody (rabbit polyclonal; Cell Signaling Technology, Danvers, MA, USA). Next we incubated the sections with species-matched fluorescence-labelled second antibodies, and observed the sections under a fluorescence or light microscope (Zeiss, Thornwood, NY, USA; Nikon, Tokyo, Japan). We counted 350–500 DRG neurons per mouse in at least three sections separated by 50 μm intervals. The number of immunopositive cells was normalised to the total number of neurons counted.

Fluorescence in situ hybridisation for Y chromosome For fluorescence in situ hybridisation (FISH) for Y chromosome, we obtained IDYE 495- or 556-labelled mouse chromosome Y paint probe from ID Labs (London, ON, Canada). We cut DRG into 10 μm sections, mounted them on gelatin-coated glass slides and incubated DRG sections or cultured DRG neurons with 0.01% pepsin solution for 20 min at 37°C. Then sections were washed with 0.1 mol/l PBS, dehydrated with ethanol and air-dried. Probes were applied to sections covered with a coverslip. Next, we co-denatured the probes and sections for 10 min at 80°C and incubated them overnight at 37°C. The coverslips were removed and slides were incubated with 50% formamide in 2×SSC (300 mmol/l NaCl, 30 mmol/l sodium citrate, pH 7.0) solution for 20 min at 37°C and

washed with 1×SSC (150 mmol/l NaCl, 15 mmol/l sodium citrate, pH 7.0) for 15 min at room temperature. We stained sections with DAPI and observed them under a laser-scanning microscope. For quantitative evaluation of nuclear ploidy, we measured DAPI intensity in whole nuclei with three-dimensional images and compared the values in cells positive and negative for Y chromosome.

Y chromosome PCR and quantification We isolated DNA from DRG using DNeasy (Qiagen). Y chromosome sequences were detected by PCR with *6y* or *Sry* sequence and standardised by *Gapdh* (sequence of primers listed in ESM Table 1) [28, 29]. For quantification of the Y chromosome, we generated standard curves of mixtures of male and female DNA from DRG tissues (male:female, by percentage: 100:0, 90:10, 80:20, 70:30, 60:40, 50:50, 40:60, 30:70, 20:80, 10:90, 0:100). DNA levels of *6y*, *Sry* and autosomal *Gapdh* were quantified by real-time PCR using PerfeCta SYBR Green SuperMix, Low ROX (Quanta Biosciences) in all samples and mixtures. The levels of *6y* and *Sry* were normalised by dividing by the autosomal *Gapdh*. Y chromosome percentages in samples were calculated from the standard curves.

TUNEL staining We fixed DRG and sciatic nerves in 4% paraformaldehyde at L3–L5, cut them into 10 μm-thick frozen sections and labelled apoptotic nuclei using a TUNEL labelling kit (Roche, Mannheim, Germany). Positive and negative controls were generated according to the kit protocol. Sections of DRG and sciatic nerves were obtained every 10 serial sections at 100 μm intervals. We evaluated 400–600 neurons/mouse and calculated the prevalence of TUNEL-positive cells in data generated from ~5 individual mice.

FACS analysis We isolated total BM cells from the femur, humerus and tibia of mice under anaesthesia. Mononuclear cells were isolated from total BM or peripheral blood cells using Ficoll-Paque (GE Healthcare Bio-Sciences, Uppsala, Sweden) and then incubated with anti-proinsulin (Fitzgerald Industries International) and anti-TNF-α antibody (Santa Cruz Biotechnology). Next we incubated the sections with species-matched fluorescence-labelled second antibodies. Data were collected using a FACS Calibur (BD Biosciences, San Jose, CA, USA).

Motor and sensory nerve conduction measurements We measured motor nerve conduction velocity (MNCV) and sensory nerve conduction velocity (SNCV) using a Sierra 6200A instrument (Cadwell, Kennewick, WA, USA) in anaesthetised mice at 30–32°C. We used sciatic nerve for motor nerve conduction measurement [30]. For sensory nerve function, we stimulated sural nerves in the distal site at ankle joint level and made recordings in the proximal site.

Statistical analysis Results are presented as means ± SD. We performed statistical analysis using SPSS Statistics 19 software (IBM SPSS, Chicago, IL, USA) and used Student's *t* test to compare two independent groups and one-way ANOVA followed by the multiple comparison test to compare three or more groups. Statistically significant difference is defined as a *p* value of <0.05.

Results

Selective loss of TNF-α expression confined to BM cells protects against diabetic neuropathy Global *Tnf* KO mice, in which TNF-α from multiple cellular sources has been ablated, were shown to be protected from the development of DPN [21]. To test the hypothesis that TNF-α-producing BM-derived cells play a key role in DPN, we performed BMT of WT vs *Tnf* KO BM into WT mice (WT→WT mice vs *Tnf* KO→WT mice). The experimental design (ESM Fig. 1a, b) consisted of transplanting BM cells from male *Tnf* KO or WT donors into WT female recipients. Four weeks after BMT, we induced diabetes with STZ (DM group); citrate buffer-injected mice served as non-diabetic WT controls (WT group). We evaluated the mice 12 weeks after STZ-induced diabetes (ESM Fig. 1a, b) and found significant hyperglycaemia and reduced body weights in both DM groups, whether they received *Tnf* KO or WT BMT, as compared with the citrate-
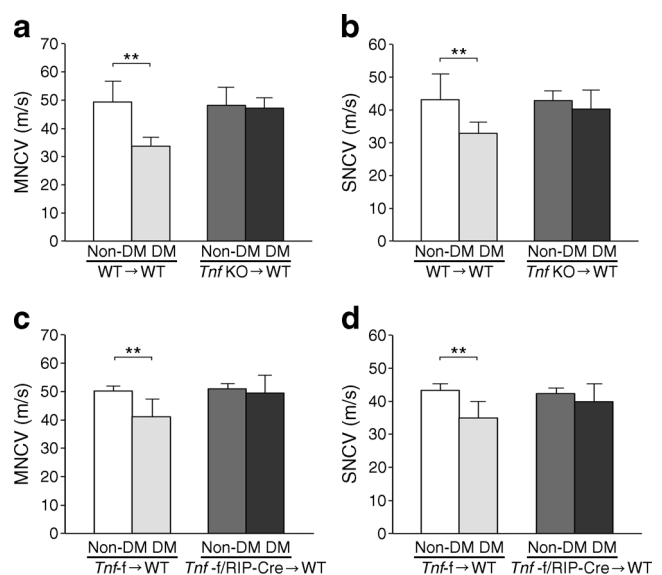
Fig. 1 Effect of *Tnf* KO BMT or loss of PI-BMDC-specific TNF-α on peripheral nerve function in STZ-diabetic mouse. MNCV (**a**, **c**) and SNCV (**b**, **d**) of mouse lower limbs. (**a**, **b**) Female WT mice were transplanted with BM from male WT (WT→WT) or *Tnf* KO (*Tnf* KO→WT) mice. (**c**, **d**) Female WT mice were transplanted with BM from male *Tnf*-flox/flox (*Tnf*-f→WT) or *Tnf*-f/RIP-Cre (*Tnf*-f/RIP-Cre→WT) mice. Data are mean ± SD, *n*=10–13; ***p*<0.01 for the indicated comparison

treated non-DM groups (ESM Fig. 1c, d). Next, we determined the MNCV (Fig. 1a) and SNCV (Fig. 1b) in DM mice and found significantly impaired velocities in mice that had received WT BM cells (DM WT→WT) compared with non-DM mice transplanted with WT BM cells (non-DM WT→WT). In contrast, there was no difference between non-DM and DM mice that had received *Tnf* KO BMT (comparing non-DM *Tnf* KO→WT and DM *Tnf* KO→WT mice). TUNEL staining detected TUNEL-positive cells only in the sections of the DM WT→WT group ($1.13\pm1.13/\text{mm}^2$, $n=6$), such cells being absent in the non-DM WT→WT group ($0.0\pm0.0/\text{mm}^2$, $n=6$); the difference between the non-DM WT→WT and DM WT→WT was significant ($p<0.05$). In contrast, there was no difference between non-DM and DM mice that had received *Tnf* KO BMT (non-DM *Tnf* KO→WT, $0.0\pm0.0/\text{mm}^2$; DM *Tnf* KO→WT, $0.14\pm0.38/\text{mm}^2$, $n=6$). Thus, selective loss of TNF-α expression only in BM-derived cells confers essentially complete protection against DPN.

PI-BMDCs are a major source of the TNF-α that underlies diabetic neuropathy Earlier studies in our laboratory suggested that PI-BMDCs are involved in the pathogenesis of DPN [30]. We therefore co-stained the sections with anti-proinsulin antibody, anti-TNF-α antibody and DAPI (nuclear staining) (Fig. 2a). In the DM WT→WT group, we detected proinsulin and TNF-α double-positive cells as previously reported [30]. We counted the immunopositive cells in the DRG and normalised the value to the total number of DRG neurons (Fig. 2b). Proinsulin-positive, TNF-α-positive and double-positive cells were significantly increased in the DM WT→WT group compared with the non-DM WT→WT group, with the double-positive cells making up ~10% of the cells 12 weeks after development of diabetes. In comparison, the proportion of proinsulin-positive cells in DM total BM was 3.25%, whereas that in non-DM BM was 0.00%. Furthermore, all proinsulin-positive cells were positive for TNF-α (data not shown). In contrast, there was no significant change in the number of proinsulin- or TNF-α-immunopositive cells in the DRG of DM *Tnf* KO→WT group when compared with the non-DM *Tnf* KO→WT group (Fig. 2b and ESM Fig. 2). We next quantified selected mRNAs in the DRG isolated from the different groups (Fig. 2c). In the DM WT→WT group, the level of *Ins1*, *Ins2* and *Tnf* transcripts was about five- to tenfold higher than in the non-DM WT→WT group. Importantly, there was no difference in the level of *Ins1*, *Ins2* and *Tnf* mRNA between DM and non-DM groups in the mice transplanted with total *Tnf* KO BM.

TNF-α expression in a specific, small and highly selective, subpopulation of BM-derived cells, PI-BMDCs, mediates diabetic neuropathy In the above BMT experiments, in which we compared the results from mice transplanted with BM

from either WT or *Tnf* KO donors, we could only infer indirectly that the pathogenic cytokine TNF-α was derived from PI-BMDCs because only a small subfraction of BM-derived cells in diabetic mice expresses proinsulin [17]. To demonstrate a direct role for PI-BMDC-derived TNF-α in the pathogenesis of DPN, we generated *Tnf*-f/RIP-Cre mice by cross-breeding *Tnf*$^{\text{flox/flox}}$ mice with RIP-Cre mice (ESM Fig. 1e) and generated PI-BMDC-specific *Tnf* conditional KO mice (*Tnf*-f/RIP-Cre→WT) by transplanting BMT from *Tnf*-f/RIP-Cre male donor mice to WT female recipient mice (ESM Fig. 1f). As control, we transplanted BM from male *Tnf*$^{\text{flox/flox}}$ (*Tnf*-f) mice to WT female mice (*Tnf*-f→WT) (ESM Fig. 1f). We induced diabetes by STZ administration in *Tnf*-f/RIP-Cre→WT and *Tnf*-f→WT mice and compared the two groups before (non-DM group) and 12 weeks after STZ treatment (DM group) (ESM Fig. 1f). Blood glucose was elevated and body weight reduced after STZ (both DM *Tnf*-f/RIP-Cre→WT and DM *Tnf*-f→WT groups) compared with the values before STZ (non-DM *Tnf*-f/RIP-Cre→WT and non-DM *Tnf*-f→WT) (ESM Fig. 1g, h).

We found that the MNCV and SNCV in the *Tnf*-f→WT group were significantly decreased at 12 weeks after STZ (DM group) compared with pre-STZ (non-DM) values (Fig. 1c, d). In contrast, neither MNCV nor SNCV in the DM *Tnf*-f/RIP-Cre→WT group was significantly different 12 weeks after STZ compared with the conduction velocities in the non-DM *Tnf*-f/RIP-Cre→WT group. We note that, under this experimental protocol, *Tnf* deletion occurs when the proinsulin promoter-driven-Cre is activated (i.e. only in PI-BMDCs). Importantly, identical results were obtained in mice transplanted with PI-BMDC-specific *Tnf* deletion BM to those obtained in mice that had received BM from global *Tnf* KO donors.

To obtain morphological evidence for proinsulin and TNF-α expression, we examined by immunocytochemistry the DRG tissue sections from DM vs non-DM *Tnf*-f/RIP-Cre→WT mice, and DM vs non-DM *Tnf*-f→WT mice (Fig. 3a). In DM *Tnf*-f→WT mice, we readily detected cells that were double-positive for proinsulin and TNF-α. In contrast, in the DM *Tnf*-f/RIP-Cre→WT group, the low rate of occurrence of such double-positive cells did not differ significantly from the number in the non-DM controls. We counted the immunopositive cells in the DRG and normalised the value to the total number of DRG neurons examined (Fig. 3b and ESM Fig. 2). The numbers of proinsulin-positive, TNF-α-positive and double-positive cells (~10%) in the DM *Tnf*-f→WT group were significantly increased compared with the numbers of such cells in non-DM *Tnf*-f→WT group. There was considerable scatter in proinsulin- or TNF-α-immunopositive cells, but the numbers did not differ between DM *Tnf*-f/RIP-Cre→WT and non-DM *Tnf*-f/RIP-Cre→WT groups. We note that the low number of single TNF-α-immunopositive cells in the DM *Tnf*-f/RIP-Cre→WT group

Fig. 2 Immunohistochemistry and mRNA expression in the DRG of global *Tnf* KO BMT mice. (**a**) Immunohistochemistry of proinsulin (green), TNF-α (red) and nucleus (DAPI, blue) in the DRG. Arrows indicate proinsulin- and TNF-α-positive cells. Scale bar, 10 μm in the magnified image and 50 μm in the other images. (**b**) Quantification of immunoreactive proinsulin and TNF-α normalised to the total number of DRG nuclei counted. Data are mean ± SD, *n*=5–10. (**c**) Levels of *Ins1*, *Ins2* and *Tnf* mRNA in the DRG quantified by real-time PCR. Results were normalised to β-actin and shown as a ratio against non-DM WT→WT group. Total RNA was extracted before and 12 weeks after STZ. Data are mean ± SD, *n*=3–8; *$p<0.05$ and **$p<0.01$ for the indicated comparison
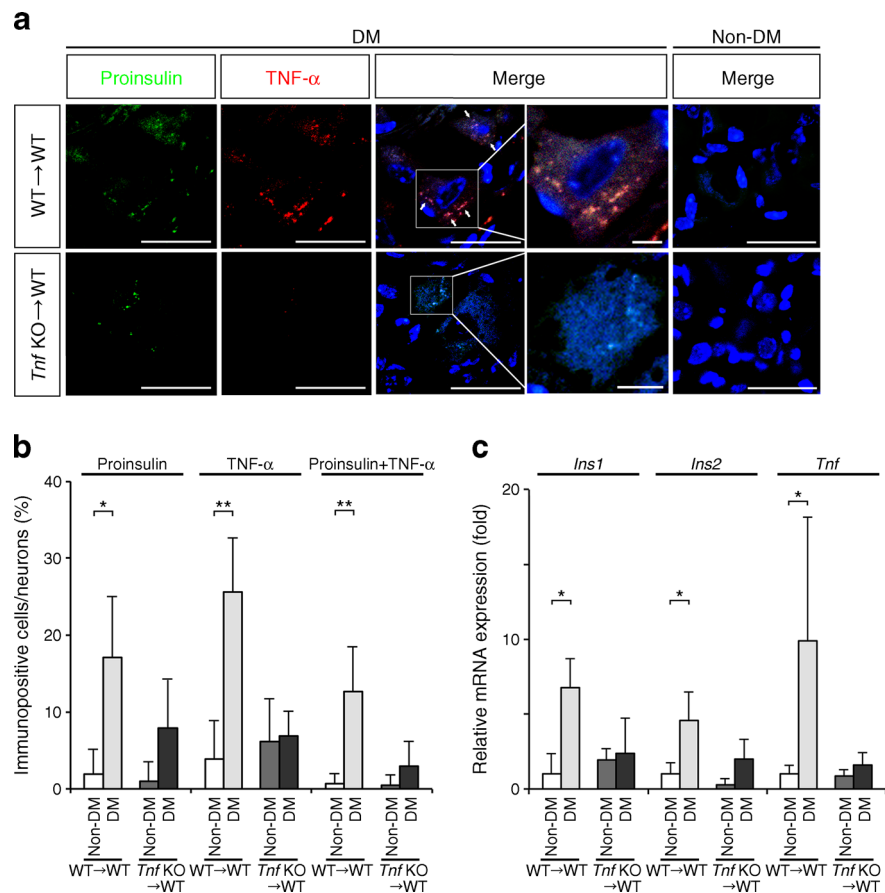
shown in Fig. 3b could have been derived from non-BM-derived neural cells and tissues, a known source of TNF-α [4, 19, 20] that is not removed by the RIP-Cre-mediated ablation strategy. The expression of TNF-α in proinsulin-positive BM cells was completely eliminated (ESM Fig. 3). To complement the immunocytochemical analysis, we quantified the mRNA level of *Ins1*, *Ins2* and *Tnf* in RNA isolated from the DRG (Fig. 3c) and found that *Ins1*, *Ins2* and *Tnf* transcripts were significantly increased in the DRG isolated from the DM *Tnf*-f→WT group as compared with the non-DM *Tnf*-f→WT group. In contrast, there was no significant difference in the levels of *Ins1*, *Ins2* or *Tnf* transcripts in the DRG isolated from non-DM vs DM *Tnf*-f/RIP-Cre→WT groups. Therefore, the data from DM *Tnf*-f/RIP-Cre→WT mice recapitulate the pattern obtained from diabetic mouse recipients of whole *Tnf* KO BM.

Next, we performed TUNEL staining to gauge the levels of apoptosis in the DRG neurons (Fig. 4a). We counted the number of TUNEL-positive cells and normalised the value to the total number of DRG neurons examined (Fig. 4b). There were few, if any, TUNEL-positive cells in the non-DM groups. The frequency of TUNEL-positive cells in the DM *Tnf*-f→WT group was much higher than in the non-DM *Tnf*-f→WT group; in contrast, there was no difference in the number of apoptotic cells between the DM and non-DM

Tnf-f/RIP-Cre→WT groups (Fig. 4a, b). Therefore, selective deletion of *Tnf* from PI-BMDCs only protects against diabetes-induced neuronal apoptosis.

TNF-α-expressing PI-BMDC–neuron fusion cells in the DRG of mice with DPN A pathogenic property of PI-BMDCs is their propensity to fuse with neurons in diabetic animals, contributing to premature apoptosis [30, 31]. Therefore, we had designed the BMT experiment in a way that enabled us to identify PI-BMDC–neuron fusion cells by transplanting BM from male donor to female recipient mice, a standard strategy for identifying fusion cells formed between BM donor cells and specific cells in the recipients [32–34]. As observed previously [24], the presence of Y chromosome genetic material within a neuron-like cell in the DRG of the recipient animal indicates a fusion cell because all DRG cells with the Y chromosome are also polyploid (ESM Fig. 4). By FISH, we detected Y chromosome-specific hybridisation signals in the nuclei of DRG neurons only in the DM *Tnf*-f→WT group (Fig. 5a) and not in the non-DM *Tnf*-f→WT, non-DM *Tnf*-f→WT, non-DM *Tnf*-f/RIP-Cre→WT or DM *Tnf*-f/RIP-Cre→WT groups.

Quantification of Y chromosome-specific sequences in DNA isolated from the DRG by real-time PCR analysis revealed a markedly higher concentration of Y chromosome

Fig. 3 Immunohistochemistry and mRNA expression in the DRG of mice with PI-BMDC-specific *Tnf* KO and controls. (**a**) Immunohistochemistry of proinsulin (green), TNF-α (red) and nuclei (DAPI, blue) in the DRG. Arrows indicate proinsulin- and TNF-α-positive cells. Scale bar, 10 μm in the magnified image and 50 μm in the other images. (**b**) Quantification of proinsulin- and TNF-α-positive cells normalised to the total number of nuclei counted. Data are mean ± SD, *n*=3–6. (**c**) Levels of *Ins1*, *Ins2* and *Tnf* mRNA in the DRG quantified by real-time PCR. Results were normalised to β-actin and shown as a ratio against non-DM WT→WT group. Total mRNA was extracted before and 12 weeks after STZ. Data are mean ± SD, *n*=3–6; †*p*=0.05, **p*<0.05 and ***p*<0.01 for the indicated comparison
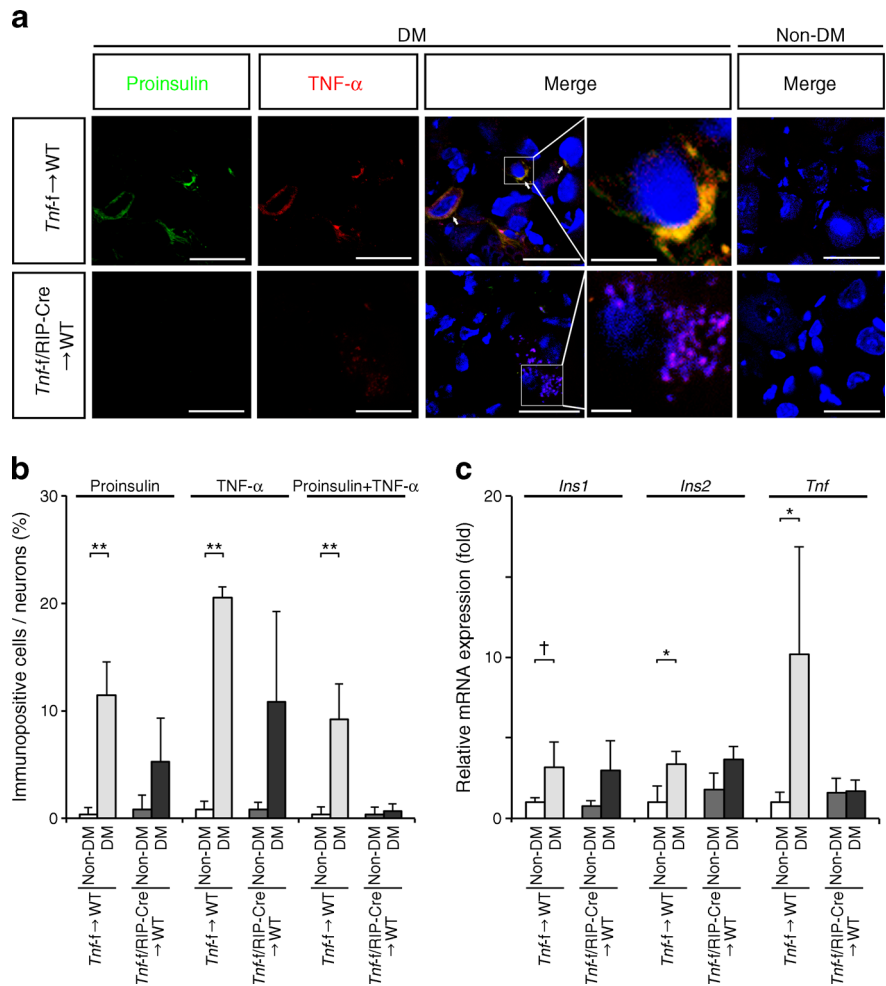
gene sequences, *6y* and *Sry*, in the DM *Tnf*-f→WT group than in the non-DM *Tnf*-f→WT group (Fig. 5b). In contrast, there was no difference in the level of Y chromosome-specific

sequences in the DM *Tnf*-f/RIP-Cre→WT group compared with the non-DM *Tnf*-f/RIP-Cre→WT group, it being very low in both (Fig. 5b). Notably, Y chromosome gene sequences detected by quantitative PCR in the DNA include low levels of BM donor DNA in the small number of BMDCs that were in transit, but not fused with neurons, in the DRG.
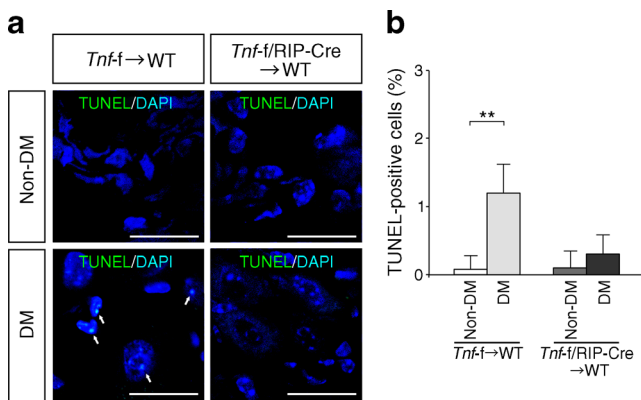
Fig. 4 TUNEL-positive cells in DRG neurons of *Tnf* conditional KO mice. (**a**) TUNEL (green) and DAPI (blue) staining of DRG before and 12 weeks after STZ. Arrows indicate TUNEL-positive cells. Scale bar, 50 μm. (**b**) Quantification of TUNEL-positive neurons in mice before and 12 weeks after STZ injection, shown as a percentage of the total number of DRG neurons examined. Data are mean ± SD, *n*=3–6; ***p*<0.01 for the indicated comparison

Discussion

A myriad of therapeutic modalities, including some in clinical trials [5], have been used to treat DPN, with limited efficacy. Unfortunately, our current understanding of the disease process is limited in our ability to rationally design novel therapeutic approaches. TNF-α is a known aetiological cytokine in DPN and is an actionable drug target [4, 19, 20]. In fact, we showed that inactivation of TNF-α using infliximab, a chimaeric monoclonal antibody for TNF-α, ameliorates DPN in mice [21]. Unfortunately, treatment of patients with autoimmune diseases with infliximab was shown to produce serious side effects (e.g. upper respiratory tract infections, urinary
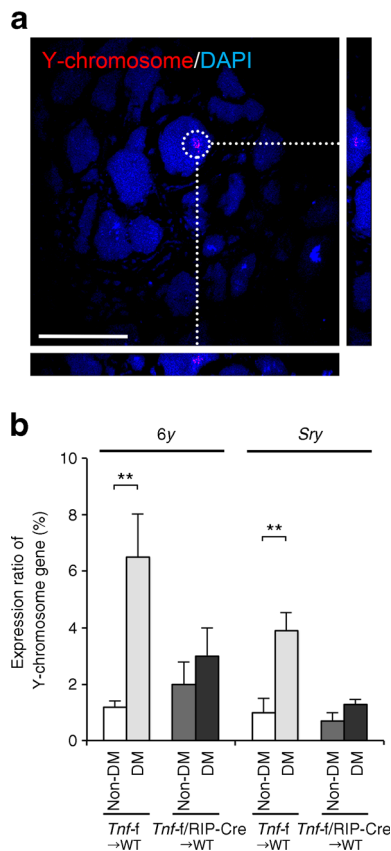
Fig. 5 Y chromosome FISH staining in the DRG of *Tnf* conditional KO BM-transplanted mice. (**a**) Y chromosome FISH (red) and DAPI (blue) staining in the DRG of DM *Tnf*-f→WT mice. Bottom and right micrographs show cross section at the white dotted circle. Y chromosome was not detected in non-DM mice or in DM *Tnf*-f/RIP-Cre→WT mice after analysis of >20 sections per group. Scale bar, 50 μm. (**b**) Quantification of *6y* and *Sry*, Y chromosome-specific sequences in the DRG of mice before and 12 weeks after STZ injection. Results were normalised to the autosomal *Gapdh* gene and calculated as relative percentage. Data are mean ± SD, *n*=3–4; **p<0.01 for the indicated comparison

tract infections) secondary to infliximab-induced immune dysfunction, as well as other adverse effects (e.g. rash, back pain, itching, fever and chills) possibly caused by allergy to the medication. Clinical trials of infliximab or similar anti-TNF-α agents in individuals with DPN have not been reported, possibly because of these potentially serious side effects.

Our laboratory has identified PI-BMDCs, which constitute ∼3% of total BM cells, as a culprit in the pathogenesis of DPN [30, 31]. PI-BMDCs are induced by hyperglycaemia and have been shown to co-express TNF-α [18]. In this study, we hypothesised that PI-BMDC-derived TNF-α is the dominant source of this pathogenic cytokine in DPN.

To address this hypothesis, we initially used BMT experiments using *Tnf* KO BMT donors and demonstrated that BM-specific loss of TNF-α protects against DPN (Figs 1a, b and 2). In fact, selective loss of TNF-α in the BM only, led to results (i.e. complete protection) that were similar to those obtained in global *Tnf* KO mice, in which there was total loss

of TNF-α produced by all tissues and cells [21]. This finding is significant because we showed that continued production of TNF-α by tissues intrinsic to the nervous system (e.g. Schwann cells and neurons [4, 19, 20]) had no significant deleterious effect on nerve function in diabetic animals, which continued to exhibit normal MNCV and SNCV (Fig. 1a, b).

BM encompasses a large heterogeneous population of cells. Diabetes was reported to compromise the function of the BM niche and BM cells [35–37]. Previous reports from our laboratory indicated that BM-derived cells may be involved in the pathogenesis of DPN [30, 31]. However, not all BM cells are necessarily perpetrators in DPN. To examine the hypothesis that the small subfraction of PI-BMDCs is the true culprit, we took advantage of the fact that PI-BMDCs produce proinsulin in response to hyperglycaemia [17, 18, 30] (i.e. the insulin gene is activated in these cells) and devised a novel strategy to inactivate TNF-α selectively in PI-BMDCs only. Therefore, transgenic mice with insulin promoter-driven Cre expression would produce Cre in all body cells that express the insulin gene in the presence of hyperglycaemia. Cross-breeding of these mice into *Tnf*-floxed mice would allow the diabetes-activated specific deletion of *Tnf* in the bigenic mice, which occurs in pancreatic beta cells as well as PI-BMDCs. To avoid the complication of *Tnf* deletion in beta cells, we used the bigenic mice as BM donors to create mice that respond to hyperglycaemia by deleting *Tnf* specifically in PI-BMDCs, leaving the TNF-α expression pattern intact in about 97% of the total BM-derived cells and in 100% of non-BMDCs (including 100% neural cells) in the diabetic recipients. Using this strategy, we found that PI-BMDC-specific TNF-α production was required for the development of DPN in STZ-diabetic mice. Of note, protection against DPN in these mice occurred (Fig. 1c, d) despite persistent hyperglycaemia.

PI-BMDCs target neural tissues for damage by their capacity to fuse with neurons and Schwann cells [30]. Indeed, by using male-to-female BMT, we demonstrated the presence of the Y chromosome as well as polyploidy in the neurons of the female diabetic BM recipients, supporting the cell fusion basis of the pathogenicity of TNF-α-expressing PI-BMDCs [30].

From a treatment standpoint, the ability to selectively inactivate the TNF-α that is expressed only by PI-BMDCs would allow us to zero in on a highly restricted therapeutic target. Instead of using anti-TNF-α reagents that annul global production of TNF-α by all body cells (which likely causes some of the side effects of the therapy), we could target the source of TNF-α that is confined to PI-BMDCs. The design of a PI-BMDC-targeted therapy in diabetes patients would require additional knowledge of the basic biology of PI-BMDCs, a research goal of our laboratory in the future. Importantly, the capacity to access PI-BMDCs could enable therapies that selectively ablate this small subfraction of

pathogenic BM cells, a novel strategy to treat/prevent DPN and possibly other chronic complications of diabetes [16].

Duality of interest The authors declare that there is no duality of interest associated with this manuscript.

Contribution statement HU contributed to the conception of the experimental design and acquisition, analysis and interpretation of data and wrote the manuscript. TT contributed to the acquisition and analysis of data and wrote the manuscript. FL contributed to the acquisition and analysis of data. HK contributed to the conception of the experimental design and interpretation of data. LC contributed to the conception of the experimental design and interpretation of data, wrote the manuscript and is the guarantor of the work. All authors reviewed the manuscript and gave final approval of the version to be published.

References

1. Brownlee M (2001) Biochemistry and molecular cell biology of diabetic complications. Nature 414:813–820
2. Yasuda H, Terada M, Maeda K et al (2003) Diabetic neuropathy and nerve regeneration. Prog Neurobiol 69:229–285
3. Hartemann A, Attal N, Bouhassira D et al (2011) Painful diabetic neuropathy: diagnosis and management. Diabetes Metab 37:377–388
4. Nguyen DV, Shaw LC, Grant MB (2012) Inflammation in the pathogenesis of microvascular complications in diabetes. Front Endocrinol 3:170
5. Vincent AM, Callaghan BC, Smith AL, Feldman EL (2011) Diabetic neuropathy: cellular mechanisms as therapeutic targets. Nat Rev Neurol 7:573–583
6. Vincent AM, Russell JW, Low P, Feldman EL (2004) Oxidative stress in the pathogenesis of diabetic neuropathy. Endocr Rev 25: 612–628
7. Schmeichel AM, Schmelzer JD, Low PA (2003) Oxidative injury and apoptosis of dorsal root ganglion neurons in chronic experimental diabetic neuropathy. Diabetes 52:165–171
8. Low PA, Lagerlund TD, McManis PG (1989) Nerve blood flow and oxygen delivery in normal, diabetic, and ischemic neuropathy. Int Rev Neurobiol 31:355–438
9. Thornalley PJ (2002) Glycation in diabetic neuropathy: characteristics, consequences, causes, and therapeutic options. Int Rev Neurobiol 50:37–57
10. Toth C, Rong LL, Yang C et al (2008) Receptor for advanced glycation end products (RAGEs) and experimental diabetic neuropathy. Diabetes 57:1002–1017
11. Xia P, Kramer RM, King GL (1995) Identification of the mechanism for the inhibition of Na+, K(+)-adenosine triphosphatase by hyperglycemia involving activation of protein kinase C and cytosolic phospholipase A2. J Clin Invest 96:733–740
12. Oates PJ (2002) Polyol pathway and diabetic peripheral neuropathy. Int Rev Neurobiol 50:325–392
13. Yagihashi S, Yamagishi SI, Wada Ri R et al (2001) Neuropathy in diabetic mice overexpressing human aldose reductase and effects of aldose reductase inhibitor. Brain J Neurol 124:2448–2458
14. Leinninger GM, Vincent AM, Feldman EL (2004) The role of growth factors in diabetic peripheral neuropathy. J Peripher Nerv Syst 9:26–53
15. Cameron NE, Cotter MA (2008) Pro-inflammatory mechanisms in diabetic neuropathy: focus on the nuclear factor kappa B pathway. Curr Drug Targets 9:60–67
16. Kojima H, Kim J, Chan L (2014) Emerging roles of hematopoietic cells in the pathobiology of diabetic complications. Trends Endocrinol Metab 25:178–187
17. Kojima H, Fujimiya M, Matsumura K, Nakahara T, Hara M, Chan L (2004) Extrapancreatic insulin-producing cells in multiple organs in diabetes. Proc Natl Acad Sci U S A 101:2458–2463
18. Fujimiya M, Kojima H, Ichinose M et al (2007) Fusion of proinsulin-producing bone marrow-derived cells with hepatocytes in diabetes. Proc Natl Acad Sci U S A 104:4030–4035
19. Satoh J, Yagihashi S, Toyota T (2003) The possible role of tumor necrosis factor-alpha in diabetic polyneuropathy. Exp Diabesity Res 4:65–71
20. Skundric DS, Lisak RP (2003) Role of neuropoietic cytokines in development and progression of diabetic polyneuropathy: from glucose metabolism to neurodegeneration. Exp Diabesity Res 4:303–312
21. Yamakawa I, Kojima H, Terashima T et al (2011) Inactivation of TNF-alpha ameliorates diabetic neuropathy in mice. Am J Physiol Endocrinol Metab 301:E844–E852
22. Shi X, Chen Y, Nadeem L, Xu G (2013) Beneficial effect of TNF-alpha inhibition on diabetic peripheral neuropathy. J Neuroinflammation 10:69
23. Liu Y, Tanabe K, Baronnier D et al (2010) Conditional ablation of Gsk-3β in islet beta cells results in expanded mass and resistance to fat feeding-induced diabetes in mice. Diabetologia 53:2600–2610
24. Terashima T, Kojima H, Chan L (2012) Bone marrow expression of poly(ADP-ribose) polymerase underlies diabetic neuropathy via hematopoietic-neuronal cell fusion. FASEB J 26:295–308
25. Poungvarin N, Lee JK, Yechoor VK et al (2012) Carbohydrate response element-binding protein (ChREBP) plays a pivotal role in beta cell glucotoxicity. Diabetologia 55:1783–1796
26. Cooke KR, Kobzik L, Martin TR et al (1996) An experimental model of idiopathic pneumonia syndrome after bone marrow transplantation: I. The roles of minor H antigens and endotoxin. Blood 88:3230–3239
27. Bryson JS, Jennings CD, Caywood BE, Dix AR, Lowery DM, Kaplan AM (1997) Enhanced graft-versus-host disease in older recipient mice following allogeneic bone marrow transplantation. Bone Marrow Transplant 19:721–728
28. Pugatsch T, Oppenheim A, Slavin S (1996) Improved single-step PCR assay for sex identification post-allogeneic sex-mismatched BMT. Bone Marrow Transplant 17:273–275
29. Peters SO, Bauermeister K, Simon JP, Branke B, Wagner T (2002) Quantitative polymerase chain reaction-based assay with fluorogenic Y-chromosome specific probes to measure bone marrow chimerism in mice. J Immunol Methods 260:109–116
30. Terashima T, Kojima H, Fujimiya M et al (2005) The fusion of bone-marrow-derived proinsulin-expressing cells with nerve cells underlies diabetic neuropathy. Proc Natl Acad Sci U S A 102:12525–12530
31. Chan L, Terashima T, Urabe H, Lin F, Kojima H (2011) Pathogenesis of diabetic neuropathy: bad to the bone. Ann N Y Acad Sci 1240:70–76
32. Weimann JM, Johansson CB, Trejo A, Blau HM (2003) Stable reprogrammed heterokaryons form spontaneously in Purkinje neurons after bone marrow transplant. Nat Cell Biol 5:959–966
33. Willenbring H, Bailey AS, Foster M et al (2004) Myelomonocytic cells are sufficient for therapeutic cell fusion in liver. Nat Med 10:744–748

34. Rizvi AZ, Swain JR, Davies PS et al (2006) Bone marrow-derived cells fuse with normal and transformed intestinal stem cells. Proc Natl Acad Sci U S A 103:6321–6325

35. Oikawa A, Siragusa M, Quaini F et al (2010) Diabetes mellitus induces bone marrow microangiopathy. Arterioscler Thromb Vasc Biol 30:498–508

36. Ferraro F, Lymperi S, Mendez-Ferrer S et al (2011) Diabetes impairs hematopoietic stem cell mobilization by altering niche function. Sci Transl Med 3:104ra101

37. Spinetti G, Cordella D, Fortunato O et al (2013) Global remodeling of the vascular stem cell niche in bone marrow of diabetic patients: implication of the microRNA-155/FOXO3a signaling pathway. Circ Res 112:510–522